

## NATURAL CONVECTION HEAT TRANSFER IN A NANOFUID FILLED INCLINED L-SHAPED ENCLOSURE<sup>\*</sup>

M. SHEIKHOESLAMI<sup>1, \*\*</sup>, M. GORJI-BANDPY<sup>2</sup>, D.D. GANJI<sup>3</sup> AND S. SOLEIMANI<sup>4</sup>

<sup>1,2,3</sup>Dept. of Mechanical Eng., Babol University of Technology, Babol, I. R. of Iran  
Email: mohsen.sheikholeslami@yahoo.com

<sup>4</sup>Dept. of Mechanical and Materials Eng., Florida International University, Miami, FL 33199

**Abstract**– In this investigation, Control Volume based Finite Element Method is applied to simulate the effects of different governing parameters on natural convection heat transfer in an inclined L-shape enclosure filled with Cu-water nanofluid. The numerical investigation is performed at a fixed Prandtl number ( $Pr$ ) equal to 6.2 and various values of non-dimensional governing parameters namely, volume fraction of nanoparticles, Rayleigh number and different inclination angles. The results show that for  $Ra = 10^4$  the maximum and minimum average Nusselt number correspond to  $\zeta = -45^\circ$  and  $45^\circ$ , respectively, whereas an opposite trend is observed for  $Ra = 10^5$ .

**Keywords**– Nanofluid, CVFEM, L-shape enclosure, natural convection, inclined enclosure

### 1. INTRODUCTION

The study of natural convection in horizontal annuli is important in many industrial and geophysical problems. This topic is of interest in several sciences such as in solar collector-receiver, underground electric transmission cables, vapor condenser for water distillation and food processing. Mohammed et al. [1] experimentally investigated the forced and free convection for thermally developing and fully developed laminar airflow inside horizontal concentric annuli. Sheikholeslami et al. [2] studied the problem of natural convection between a circular enclosure and a sinusoidal cylinder. They concluded that streamlines, isotherms, and the number, size and formation of the cells inside the enclosure strongly depend on the Rayleigh number, values of amplitude and the number of undulations of the enclosure. Xu et al. [3] have studied laminar convection heat transfer from a horizontal triangular cylinder to its concentric cylindrical enclosure. They indicated that at constant aspect ratio, both the inclination angle and cross-section geometry have insignificant effects on the overall heat transfer rates.

In most of the available studies on natural convection in enclosures, the base fluid is a common fluid for which the thermal conductivity is usually low. The resulting performances of such thermal systems are thus relatively poor. A recent way of improving the performance of these systems is to suspend metallic nanoparticles in the base fluid. Khanafer et al. [4] firstly conducted a numerical investigation on the heat transfer enhancement due to adding nano-particles in a differentially heated enclosure. Sheikholeslami et al. [5] used heatline analysis to investigate two phase simulation of nanofluid flow and heat transfer. Their results indicated that the average Nusselt number decreases as buoyancy ratio number increases until it reaches a minimum value and then starts increasing. Rashidi et al. [6] considered the analysis of the

---

\*Received by the editors May 28, 2013; Accepted November 2, 2013.

\*\*Corresponding author

second law of thermodynamics applied to an electrically conducting incompressible nanofluid flowing over a porous rotating disk. Free convection heat transfer in a concentric annulus between a cold square and heated elliptic cylinders in presence of magnetic field was investigated by Sheikholeslami et al. [7]. They found that the enhancement in heat transfer increases as Hartmann number increases but it decreases with increase of Rayleigh number. Sheikholeslami et al. [8] used the lattice Boltzmann method to examine free convection of nanofluids. They found that choosing copper as the nanoparticle leads to obtaining the highest enhancement for this problem. Also, their results indicate that the maximum value of enhancement occurs in  $\lambda = 2.5$  at  $Ra = 10^6$  while for other Rayleigh numbers it is obtained at  $\lambda = 1.5$ . Nabi and Shirani [9] considered Brownian motion of nanoparticles and clusters and resulted micromixing are combined with the aggregation kinetics of clusters to capture the effects of nanoparticles on the thermal conductivity of nanofluids.

Control Volume based Finite Element Method (CVFEM) is a scheme that uses the advantages of both finite volume and finite element methods for simulation of multi-physics problems in complex geometries [10]. Soleimani et al. [11] studied natural convection heat transfer in a semi-annulus enclosure filled with nanofluid using the Control Volume based Finite Element Method. They found that the angle of turn has an important effect on the streamlines, isotherms and maximum or minimum values of local Nusselt number. Sheikholeslami et al. [12] performed a numerical analysis for natural convection heat transfer of Cu-water nanofluid in a cold outer circular enclosure containing a hot inner sinusoidal circular cylinder in presence of horizontal magnetic field. They found that the average Nusselt number is an increasing function of nanoparticle volume fraction, the number of undulations and Rayleigh numbers while it is a decreasing function of Hartmann number. Sheikholeslami et al. [13] used CVFEM to simulate the effect of a magnetic field on natural convection in an inclined half-annulus enclosure filled with Cu-water nanofluid. Their results indicated that Hartmann number and the inclination angle of the enclosure can be considered as control parameters at different Rayleigh number.

The main goal of the present work is to conduct a numerical investigation of natural convection heat transfer in an L-shape inclined enclosure filled with nanofluid using the CVFEM. The numerical investigation is carried out for different governing parameters such as the Rayleigh number, volume fraction of nanoparticles and inclination angles.

## 2. GEOMETRY DEFINITION AND BOUNDARY CONDITIONS

The physical model along with the important geometrical parameters and the mesh of the enclosure used in the present CVFEM program are shown in Fig. 1a,b. To assess the shape of inner circular and outer rectangular boundary which consists of the right and top walls, a super elliptic function can be used as follows:

$$\left(\frac{X}{a}\right)^{2n} + \left(\frac{Y}{b}\right)^{2n} = 1 \quad (1)$$

When  $a = b$  and  $n = 1$  the geometry becomes a circle. As  $n$  increases from 1 the geometry would approach a rectangle for  $a \neq b$  and square for  $a = b$ .

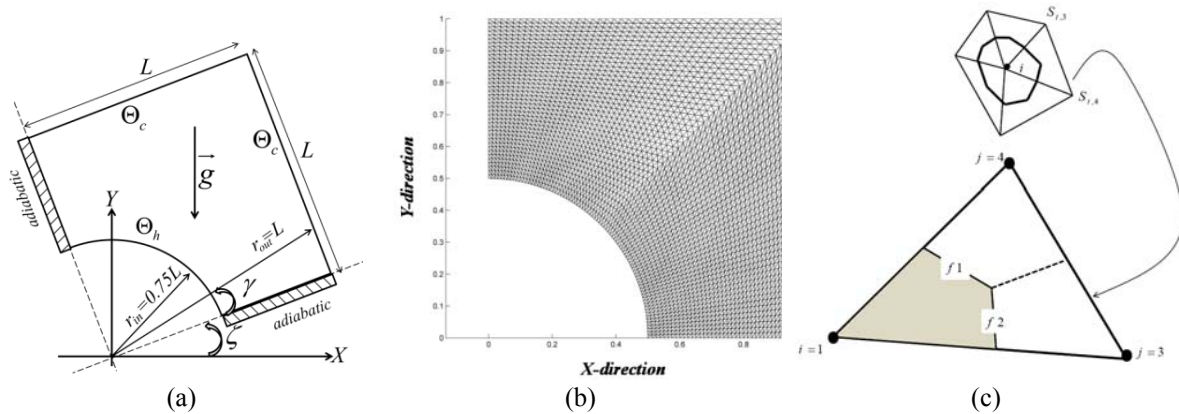


Fig. 1. (a)Geometry and the boundary conditions with (b) the mesh of enclosure considered in this work; (c) A sample triangular element and its corresponding control volume

### 3. MATHEMATICAL MODELING AND NUMERICAL PROCEDURE

#### a) Problem formulation

According to [13] non dimensional governing equations are as follows:

$$\frac{\partial \Psi}{\partial Y} \frac{\partial \Omega}{\partial X} - \frac{\partial \Psi}{\partial X} \frac{\partial \Omega}{\partial Y} = Pr_f / [(1-\phi)^{2.5} \left( (1-\phi) + \phi \frac{\rho_s}{\rho_f} \right)] \left( \frac{\partial^2 \Omega}{\partial X^2} + \frac{\partial^2 \Omega}{\partial Y^2} \right) \quad (2)$$

$$+ Ra_f Pr_f \left[ (1-\phi) + \phi \frac{\beta_s}{\beta_f} \right] \left( \frac{\partial \Theta}{\partial X} \right)$$

$$\frac{\partial \Psi}{\partial Y} \frac{\partial \Theta}{\partial X} - \frac{\partial \Psi}{\partial X} \frac{\partial \Theta}{\partial Y} = k_f / \left[ (1-\phi) + \left( (1-\phi) + \phi \frac{(\rho C_p)_s}{(\rho C_p)_f} \right) \right] \left( \frac{\partial^2 \Theta}{\partial X^2} + \frac{\partial^2 \Theta}{\partial Y^2} \right) \quad (3)$$

$$\frac{\partial^2 \Psi}{\partial X^2} + \frac{\partial^2 \Psi}{\partial Y^2} = -\Omega \quad (4)$$

The boundary conditions as shown in Fig. 1(a) are:

$$\begin{aligned} \Theta &= 1.0 && \text{on the inner circular boundary} \\ \Theta &= 0.0 && \text{on the outer walls boundary} \\ \partial \Theta / \partial n &= 0.0 && \text{on two other insulation boundaries} \\ \Psi &= 0.0 && \text{on all solid boundaries} \end{aligned} \quad (5)$$

The values of vorticity on the boundary of the enclosure can be obtained using the stream function formulation and the known velocity conditions during the iterative solution procedure. The local Nusselt number of the nanofluid along the hot wall can be expressed as:

$$Nu_{loc} = \left( \frac{k_{nf}}{k_f} \right) \frac{\partial \Theta}{\partial r} \quad (6)$$

where \$r\$ is the radial direction. The average Nusselt number on hot circular wall is evaluated as:

$$Nu_{ave} = \frac{1}{0.5\pi} \int_0^{0.5\pi} Nu_{loc}(\zeta) d\zeta \quad (7)$$

**b) Numerical procedure**

A control volume finite element method is used in this work. The building block of the discretization is the triangular element and the values of variables are approximated with linear interpolation within the elements. The control volumes are created by joining the center of each element in the support to the mid points of the element sides that pass through the central node  $i$  which creates a close polygonal control volume (see Fig. 1 (b)). The set of governing equations is integrated over the Control Volume with the use of linear interpolation inside the finite element and the obtained algebraic equations are solved by the Gauss-Seidel Method. A FORTRAN code is developed to solve the present problem using a structured mesh of linear triangular ([13]).

**4. GRID TESTING AND CODE VALIDATION**

A mesh testing procedure was conducted to guarantee the grid-independency of the present solution. Various mesh combinations were explored for the case of  $Ra = 10^5$ ,  $\phi = 0.06$ ,  $Pr = 6.2$  and  $\zeta = 0^\circ$  as shown in Table 2. The present code was tested for grid independence by calculating the average Nusselt number on the inner circular wall. In agreement with this, it was found that a grid size of  $71 \times 211$  ensures a grid-independent solution. The convergence criterion for the termination of all computations is:

$$\max_{grid} |\Gamma^{n+1} - \Gamma^n| \leq 10^{-7} \tag{8}$$

where  $n$  is the iteration number and  $\Gamma$  stands for the independent variables ( $\Omega, \Psi, \Theta$ ). The present numerical solution is validated by comparing the results of the present code against the results of experimental study of Kuehn and Goldstein [14], Labonai and Guj [15] at the different Rayleigh numbers as shown in Fig. 2(a,b). In addition, Fig. 2 illustrates an excellent agreement between the present calculations and the results of Khanafer et al. [4] for natural convection in an enclosure filled with Cu-water nanofluid. Also this method is applied in different problems [16-23].

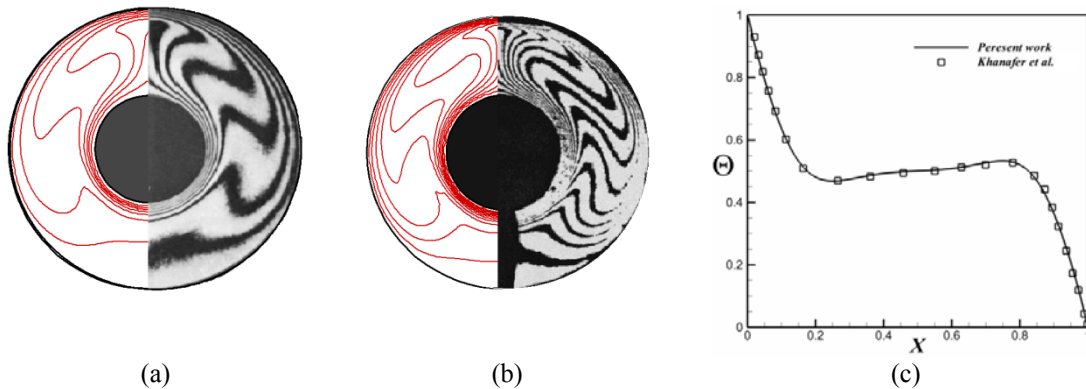


Fig. 2. Comparison of isotherms between the present work (left) and experimental study (right) of (a) Kuehn and Goldstein [14]; and Laboni and Guj [15] for viscous flow ( $\phi = 0, Pr = 0.71$ ) when (a)  $R_o / R_i = 2.6, Ra = 4.7 \times 10^4$ ; (b)  $R_o / R_i = 2.36, Ra = 0.9 \times 10^5$ . (c) Comparison of the temperature on axial midline between the present results and numerical results obtained by Khanafer et al. [4] for  $Gr = 10^4$ ,  $\phi = 0.1$  and  $Pr = 6.2$  (Cu - Water)

Table 1. Thermo physical properties of water and nanoparticles [4]

	$\rho$ (kg / m <sup>3</sup> )	$C_p$ (j / kgk)	$k$ (W / m.k)	$\beta \times 10^5$ (K <sup>-1</sup> )
Pure water	997.1	4179	0.613	21
Copper (Cu)	8933	385	401	1.67

Table 2. Comparison of the average Nusselt number  $Nu_{ave}$  for different grid resolution at  $Ra = 10^5$ ,  $\phi = 0.06$ ,  $Pr = 6.2$  and  $\zeta = 0^\circ$

Mesh size	41×121	51×151	61×181	71×211	81×241
$Nu_{ave}$	7.542921	7.531866	7.514557	7.496777	7.480536

## 5. RESULTS AND DISCUSSION

In this study, natural convection heat transfer in an L-shape inclined enclosure filled with Cu-water nanofluid is investigated. Calculations are made for various values of volume fraction of nanoparticles ( $\phi = 0\%, 2\%, 4\%$  and  $6\%$ ), Rayleigh number ( $Ra = 10^3, 10^4$  and  $10^5$ ), different inclination angles ( $\zeta = -45^\circ, 0^\circ$  and  $45^\circ$ ) and constant Prandtl number ( $Pr = 6.2$ ).

Comparison of the isotherms and streamlines contours for different values of Rayleigh numbers and inclination angles at  $\phi = 0.06$  is shown in Fig. 3. At  $Ra = 10^3$  the isotherms are parallel to each other and take the shape of enclosure which is the main characteristic of conduction heat transfer mechanism. As Rayleigh number increases the isotherms become more distorted and the stream function values enhance which is due to the domination of convective heat transfer mechanism at higher Rayleigh numbers. At  $Ra = 10^3$  and  $10^4$  the maximum value of stream function occurs at  $\zeta = -45^\circ$  while this maximum value corresponds to  $\zeta = 0^\circ$  at  $Ra = 10^5$ . At  $\zeta = 45^\circ$  the temperature contours and streamlines are symmetric with respect to the vertical lines which pass through the corner of the enclosure. It is due to the existence of symmetric boundary condition and geometry of the cavity with respect to this line. At  $\zeta = -45^\circ$  and  $0^\circ$  increase of Rayleigh number causes the thermal boundary layer thickness on the hot circular wall to decrease near the bottom wall of the enclosure, hence it is predictable that the local Nusselt number obtains its minimum value at this area. The isotherms show that at  $Ra = 10^4$ , a thermal plume appears over the hot surface at  $\gamma = 45^\circ$ . At this inclination angle, when  $Ra$  increases up to  $10^5$  the thermal plume grows and impinges the hot fluid to the cold walls of the cavity.

Figure 4 shows the distribution of local Nusselt numbers along the surface of the inner circular wall for different inclination angles, Rayleigh numbers and nanoparticle volume fractions. For all values of  $\zeta$ , increasing the nanoparticle volume fraction and Rayleigh number lead to an increase in local Nusselt number. The sensitivity of thermal boundary layer thickness to volume fraction of nanoparticles is related to the increased thermal conductivity of the nanofluid. In fact, higher values of thermal conductivity are accompanied by higher values of thermal diffusivity. The high value of thermal diffusivity causes a drop in the temperature gradients and accordingly increases the boundary thickness. This increase in thermal boundary layer thickness reduces the Nusselt number, however, the Nusselt number is a multiplication of temperature gradient and the thermal conductivity ratio (conductivity of the of the nanofluid to the conductivity of the base fluid). Since the reduction in temperature gradient due to the presence of nanoparticles is much smaller than thermal conductivity ratio an enhancement in Nusselt takes place by increasing the volume fraction of nanoparticles. At  $Ra = 10^3$ , because of domination conduction heat transfer mechanism, the distribution of the local Nusselt numbers along the surface of inner circular show a symmetric shape. Also, it can be found that as Rayleigh number increases the location of the minimum local Nusselt number approaches  $\gamma = 45^\circ$ .

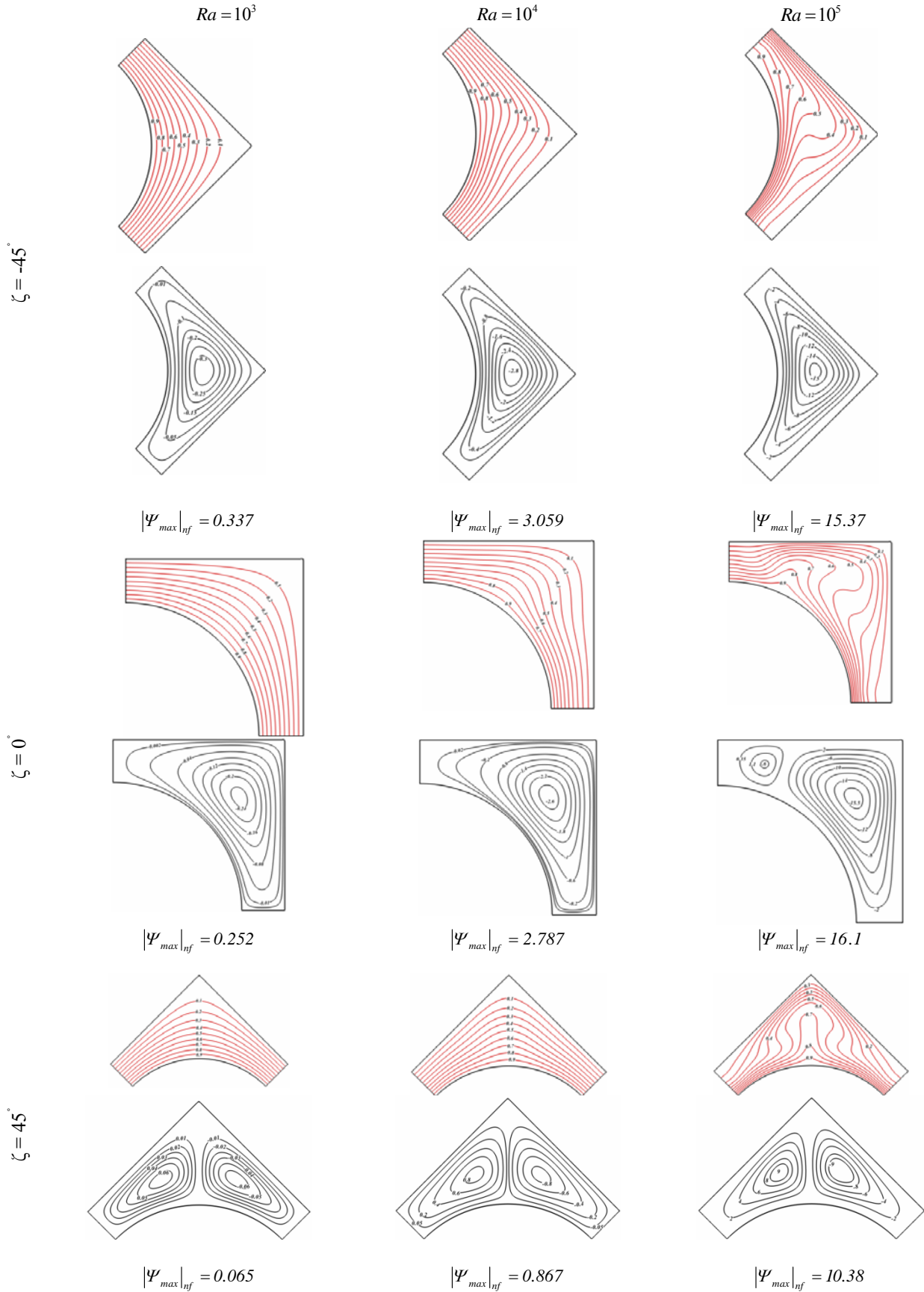


Fig. 3. Comparison of the isotherms (up) and streamlines (down) contours for different values of Rayleigh numbers and inclined angles at  $\phi = 0.06$

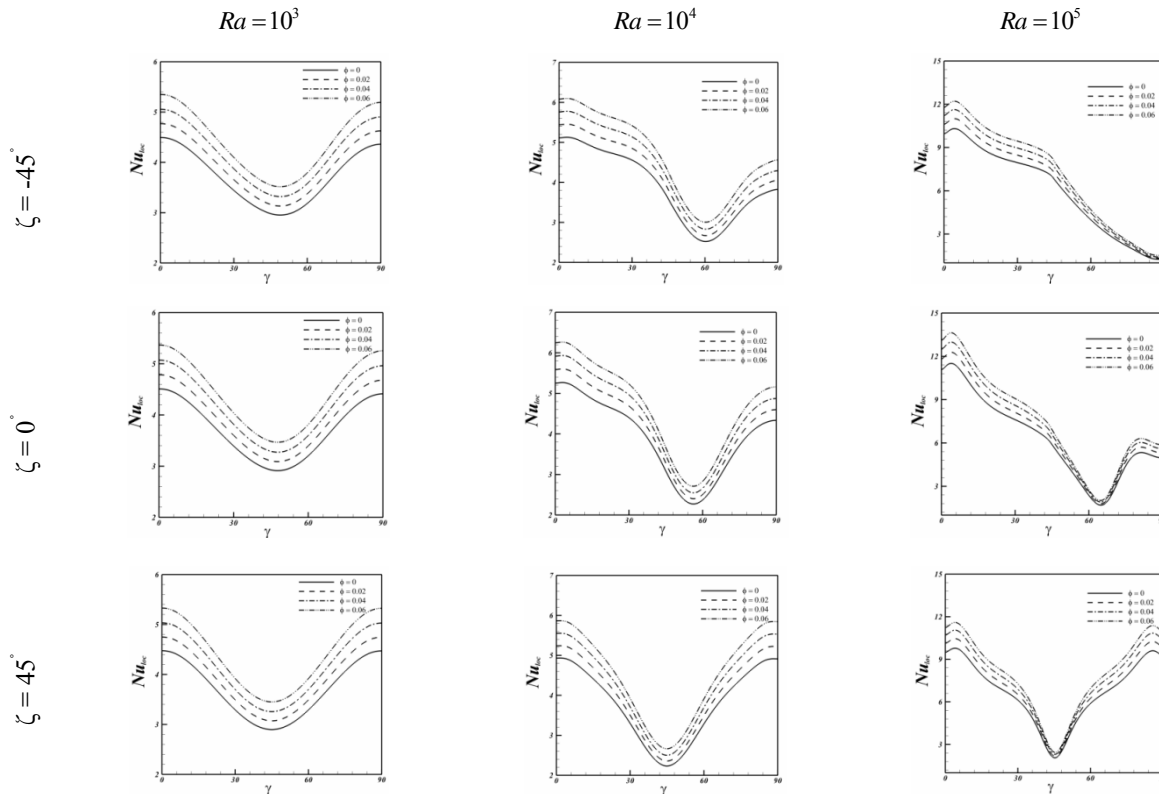


Fig. 4. Effects of the nanoparticle volume fraction, Rayleigh number and inclined angle for Cu-water nanofluids on Local Nusselt number

Figure 5a shows the effects of Rayleigh number and inclination angle for Cu-water nanofluids on average Nusselt number. Effect of inclination angle on  $Nu_{ave}$  is more pronounced at higher Rayleigh number. At  $Ra=10^4$  the maximum and minimum average Nusselt number correspond to  $\zeta = -45^\circ$  and  $45^\circ$ , respectively, but opposite trend is observed for  $Ra=10^5$ . The corresponding polynomial representation of such model for Nusselt number is as follows:

$$Nu_{ave} = a_{12} + a_{22}\zeta + a_{32}Y_1 + a_{42}\zeta^2 + a_{52}Y_1^2 + a_{62}\zeta Y_1 \tag{9}$$

$$Y_1 = a_{11} + a_{21} \log(Ra) + a_{31}\phi + a_{41} (\log(Ra))^2 + a_{51}\phi^2 + a_{61} \log(Ra)\phi$$

Also,  $a_{ij}$  can be found in Table 3, for example  $a_{21}$  is equal to (-8.82292).

Table 3. Constant coefficient for using Eq. (9)

$a_{ij}$	i=1	i=2	i=3	i=4	i=5	i=6
j=1	18.78013	-8.82292	-0.78209	1.26897	-4.50225	3.891385
j=2	0.587531	-0.85228	0.77581	-0.01719	0.02018	0.198365

To estimate the enhancement of heat transfer between the case of  $\phi = 0.06$  and the pure fluid (base fluid) case, the enhancement is defined as:

$$E = \frac{Nu(\phi = 0.06) - Nu(basefluid)}{Nu(basefluid)} \times 100 \tag{10}$$

The heat transfer enhancement ratio due to addition of nanoparticles for different values of  $\zeta$  and  $Ra$  is shown in Fig. 5b. It can be found that the effect of nanoparticles is more pronounced at low Rayleigh number than at high Rayleigh number because of the greater enhancement rate. This observation can be explained by noting that at low Rayleigh number the heat transfer is dominant by conduction. Therefore, the addition of high thermal conductivity nanoparticles will increase the conduction and make the

enhancement more effective. It is an interesting observation that the enhancement in heat transfer for at  $Ra = 10^3$  is the same for all inclination angles. Also, for  $Ra = 10^4$  and  $10^5$ , minimum value of enhancement is obtained at  $\zeta = 0^\circ$ .

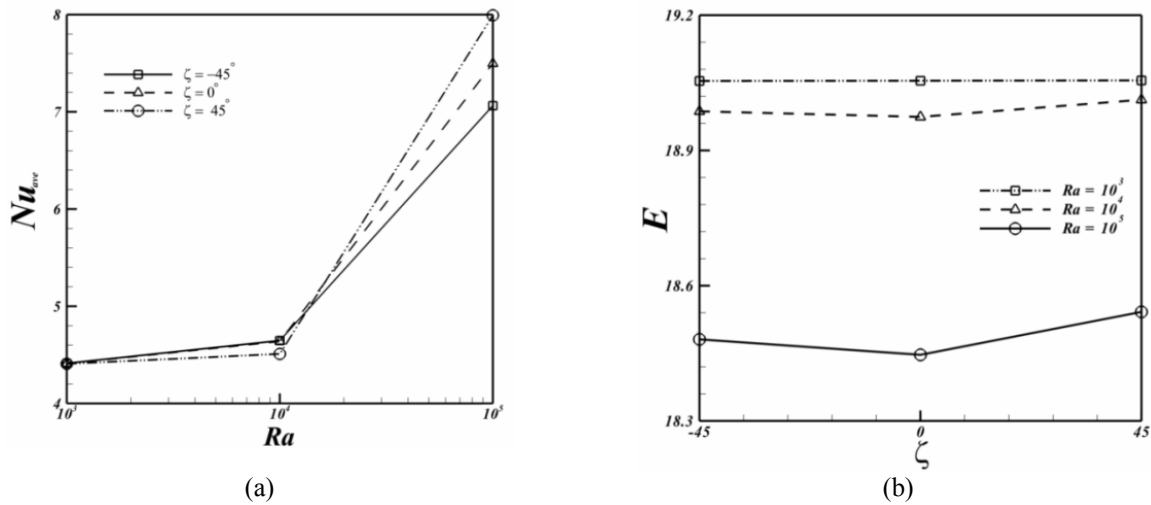


Fig. 5. (a) Effects of Rayleigh number and inclination angle for Cu-water nanofluids on average Nusselt number at  $\phi = 0.06$ ; (b) Effects of Rayleigh number and inclination angle for Cu-water nanofluids on the ratio of heat transfer enhancement due to addition of nanoparticles

## 6. CONCLUSION

In this study, natural convection heat transfer in an inclined L-shape enclosure filled with nanofluid with a circular hot wall is investigated using CVFEM. From the numerical investigation, it can be concluded that the inclination angle of the enclosure can be a control parameter for heat and fluid flow. Also, a correlation of Nusselt number corresponding to active parameters is presented. The results reveal that average Nusselt number is an increasing function of nanoparticle volume fraction and Rayleigh number. Effect of inclination angle on average Nusselt number is more pronounced at higher Rayleigh number. It can be found that the effect of nanoparticles is more pronounced at low Rayleigh number than at high Rayleigh number because of the domination of Nusselt number. In addition, the enhancement in heat transfer for at  $Ra = 10^3$  is the same for all inclination angles. Also, for  $Ra = 10^4$  and  $10^5$ , minimum value of enhancement is obtained at  $\zeta = 0^\circ$ .

## NOMENCLATURE

$C_p$	specific heat at constant pressure	$\alpha$	thermal diffusivity
$Gr_f$	Grashof number	$\phi$	volume fraction
$Nu$	Nusselt number	$\mu$	dynamic viscosity
$Pr$	Prandtl number ( $= \nu_f / \alpha_f$ )	$\nu$	kinematic viscosity
$T$	fluid temperature	$\psi$ & $\Psi$	stream function & dimensionless stream function
$u, v$	velocity components in the x-direction and y-direction	$\Theta$	dimensionless temperature
$U, V$	dimensionless velocity components in the X-direction and Y-direction	$\rho$	fluid density
$x, y$	space coordinates	$\beta$	thermal expansion coefficient
$X, Y$	dimensionless space coordinates	<b>Subscripts</b>	
$r$	non-dimensional radial distance	$c$	cold



$k$	thermal conductivity	$h$	hot
$L$	gap between inner and outer boundary of the enclosure $L = r_{out} - r_{in}$	$loc$	local
$\vec{g}$	gravitational acceleration vector	$ave$	average
$Ra$	Rayleigh number $(= g \beta_f L^3 (T_h - T_c) / (\alpha_f \nu_f))$	$nf$	nanofluid
<b>Greek symbols</b>		$f$	base fluid
$\gamma$	angle measured from right plane	$s$	solid particles
$\zeta$	inclination angle	$in$	inner
		$out$	outer

## REFERENCES

1. Mohammed, H. A. Campo, A. & Saidur, R. (2010). Experimental study of forced and free convective heat transfer in the thermal entry region of horizontal concentric annuli. *International Commu Heat and Mass Trans*, Vol. 37, pp. 739–747.
2. Sheikholeslami, M., Gorji-Bandpy, M., Pop, I. & Soleimani, S. (2013). Numerical study of natural convection between a circular enclosure and a sinusoidal cylinder using control volume based finite element method. *International Journal of Thermal Sciences*, Vol. 72, pp. 147-158.
3. Xu, X., Yu, X., Hu, Y., Fan, L. & Cen, K. (2010). A numerical study of laminar natural convective heat transfer around a horizontal cylinder inside a concentric air-filled triangular enclosure. *International Journal of Heat and Mass Transfer*, Vol. 53, pp. 345–355.
4. Khanafer, K., Vafai, K. & Lightstone, M. (2003). Buoyancy-driven heat transfer enhancement in a two-dimensional enclosure utilizing nanofluids. *Int. J. Heat Mass Transfer*, Vol. 46, pp. 3639–3653.
5. Sheikholeslami, M., Gorji-Bandpy, M. & Soleimani, S. (2013). Two phase simulation of nanofluid flow and heat transfer using heatline analysis. *International Communications in Heat and Mass Transfer*, Vol. 47, pp. 73–81.
6. Rashidi, M. M., Abelman, S. & Freidooni Mehr, N. (2013). Entropy generation in steady MHD flow due to a rotating porous disk in a nanofluid. *International Journal of Heat and Mass Transfer*, Vol. 62, pp. 515–525.
7. Sheikholeslami, M., Gorji-Bandpy, M. & Ganji, D. D. (2013). Numerical investigation of MHD effects on Al<sub>2</sub>O<sub>3</sub>-water nanofluid flow and heat transfer in a semi-annulus enclosure using LBM. *Energy*, Vol. 60, pp. 501-510.
8. Sheikholeslami, M., Gorji-Bandpy, M. & Domairry, G. (2013). Free convection of nanofluid filled enclosure using lattice Boltzmann method (LBM). *Appl. Math. Mech. -Engl. Ed.*, Vol. 34, No. 7, pp. 1–15.
9. Nabi, S. & Shirani, E. (2012), Simultaneous effects of brownian motion and clustering of nanoparticles on thermal conductivity of nanofluids. *Iranian Journal of Science & Technology, Transactions of Mechanical Engineering*, Vol. 36, No. M1, pp 53-68.
10. Voller, V. R. (2009). *Basic control volume finite element methods for fluids and solids*, World Scientific Publishing Co. Pte. Ltd. 5 Tohccxxvc.
11. Soleimani, S., Sheikholeslami, M., Ganji, D.D. & Gorji-Bandpay, M. (2012). Natural convection heat transfer in a nanofluid filled semi-annulus enclosure. *International Communications in Heat and Mass Transfer*, Vol. 39, pp. 565–574.
12. Sheikholeslami, M., Gorji-Bandpy, M., Ganji, D. D., Soleimani, S. & Seyyedi, S. M. (2012). Natural convection of nanofluids in an enclosure between a circular and a sinusoidal cylinder in the presence of magnetic field. *International Communications in Heat and Mass Transfer*, Vol. 39, pp. 1435–1443.

13. Sheikholeslami, M., Gorji-Bandpy, M., Ganji, D. D. & Soleimani, S. (2013). Effect of a magnetic field on natural convection in an inclined half-annulus enclosure filled with Cu–water nanofluid using CVFEM. *Advanced Powder Technology*, doi.org/10.1016/j.appt.2013.01.012.
14. Kuehn, T. H. & Goldstein, R. J. (1976). An experimental and theoretical study of natural convection in the annulus between horizontal concentric cylinders. *Journal of Fluid Mechanics*, Vol. 74, pp. 695-719.
15. Laboni, G. & Guj, G. (1998) Natural convection in a horizontal concentric cylindrical annulus: oscillatory flow and transition to chaos. *Journal of Fluid Mechanics*, Vol. 375, pp. 179-202.
16. Sheikholeslami, M., Gorji-Bandpy, M., Ganji, D. D., Rana, P. & Soleimani, S. (2014). Magnetohydrodynamic free convection of Al<sub>2</sub>O<sub>3</sub>-water nanofluid considering Thermophoresis and Brownian motion effects. *Computers & Fluids*, Vol. 94, pp. 147–160.
17. Sheikholeslami, M., Gorji-Bandpy, M., Ganji, D. D. & Soleimani, S. (2014). Thermal management for free convection of nanofluid using two phase model. *Journal of Molecular Liquids*, Vol. 194, pp. 179–187.
18. Sheikholeslami, M., Gorji-Bandpy, M., Ganji, D. D. & Soleimani, S. (2014). Heat flux boundary condition for nanofluid filled enclosure in presence of magnetic field. *Journal of Molecular Liquids*, Vol. 193, pp. 174-184.
19. Sheikholeslami, M., Gorji-Bandpy, M., Ganji, D. D. & Soleimani, S. (2014). Magnetic field effect on nanofluid flow and heat transfer using KKL model. *Journal of the Taiwan Institute of Chemical Engineers*, Vol. 45, pp. 795–807.
20. Sheikholeslami, M., Gorji Bandpy, M., Ellahi, R., Hassan, M. & Soleimani, S. (2014). Effects of MHD on Cu-water nanofluid flow and heat transfer by means of CVFEM. *Journal of Magnetism and Magnetic Materials*, Vol. 349, pp. 188–200.
21. Sheikholeslami, M., Gorji-Bandpy, M., Ganji, D. D. & Soleimani, S. (2014). Natural convection heat transfer in a cavity with sinusoidal wall filled with CuO-water nanofluid in presence of magnetic field. *Journal of the Taiwan Institute of Chemical Engineers*, Vol. 45, pp. 40–49.
22. Sheikholeslami, M., Hashim, I. & Soleimani, S. (2013). Numerical investigation of the effect of magnetic field on natural convection in a curved-shape enclosure. Hindawi Publishing Corporation Mathematical Problems in Engineering, Article ID 831725, 11 pages <http://dx.doi.org/10.1155/2013/831725>.
23. Sheikholeslami, M., Gorji-Bandpy, M., Ganji, D. D. & Soleimani, S. (2014). MHD natural convection in a nanofluid filled inclined enclosure with sinusoidal wall using CVFEM. *Neural Comput & Applic*, Vol. 24, pp. 873–882.